Published in final edited form as:
Dev Biol. 2008 September 15; 321(2): 446–454. doi:10.1016/j.ydbio.2008.05.551.

Regulation of the feedback antagonist *naked cuticle* by Wingless signaling

Jinhee L. Chang[1], **Mikyung V. Chang**[1], **Scott Barolo**[2], and **Ken M. Cadigan**[1]

[1]Department of Molecular, Cellular and Developmental Biology, University of Michigan, 830 N. University Ave. Ann Arbor MI 48109-1048

[2]Department of Cell and Developmental Biology, University of Michigan Medical School, 109 Zina Pitcher Place, Ann Arbor, MI 48109-2200

Abstract

Signaling pathways usually activate transcriptional targets in a cell type-specific manner. Notable exceptions are pathway-specific feedback antagonists, which serve to restrict the range or duration of the signal. These factors are often activated by their respective pathways in a broad array of cell types. For example, the Wnt ligand Wingless (Wg) activates the *naked cuticle (nkd)* gene in all tissues examined throughout *Drosophila* development. How does the *nkd* gene respond in such an unrestricted manner to Wg signaling? Analysis in cell culture revealed regions of the *nkd* locus that contain Wg response elements (WREs) that are directly activated by the pathway via the transcription factor TCF. In flies, Wg signaling activates these WREs in multiple tissues, in distinct but overlapping patterns. These WREs are necessary and largely sufficient for *nkd* expression in late stage larval tissues, but only contribute to part of the embryonic expression pattern of *nkd*. These results demonstrate that *nkd* responsiveness to Wg signaling is achieved by several WREs which are broadly (but not universally) activated by the pathway. The existence of several WREs in the *nkd* locus may have been necessary to allow the Wg signaling-Nkd feedback circuit to remain intact as Wg expression diversified during animal evolution.

Keywords

naked cuticle; feedback antagonist; Wnt; TCF; Wingless

Introduction

Throughout development, some signaling pathways are used in a reiterated manner to achieve the proper regulation of gene expression. For example, the *Drosophila* gene *wingless* (*wg*), which encodes a member of the Wnt family of secreted signaling proteins, has numerous essential roles in embryogenesis and larval stages (Couso et al., 1993; Klingensmith and Nusse, 1994). Because Wg signaling so profoundly affects cell fate, its expression is tightly controlled both spatially and temporally (Couso et al., 1993; Sanson, 2001). To achieve this complex pattern of expression, the *wg* locus contains multiple enhancers, each active in different tissues

*Corresponding author. Fax: 1 734 647 0884, *E-mail address*: cadigan@umich.edu (K.M. Cadigan).

and controlled by various signal and local inputs (Costas et al., 2004; Lessing and Nusse, 1998; Neumann and Cohen, 1996; Pereira et al., 2006).

The Wg ligand is the trigger for an evolutionarily conserved signaling cascade that promotes nuclear accumulation of the fly β-catenin, Armadillo (Arm). Nuclear Arm binds to the transcription factor TCF, converting it from a transcriptional repressor to an activator of Wg targets (Parker et al., 2007; Stadeli et al., 2006). Consistent with its multitude of functions, Wg signaling regulates gene expression in a cell and tissue-specific manner. For example, in the embryo, epidermal Wg activates Engrailed (En) and Hedgehog expression in the epidermis (Sanson, 2001) but mesodermal Wg regulates a different set of targets in the visceral and cardiac mesoderm (Bilder and Scott, 1998; Riese et al., 1997). In wing imaginal discs, Wg signaling regulates a different set of targets (Cadigan, 2002). The specificity of Wg activation is thought to occur through combinatorial regulation with other factors or signaling pathways. For example, the Wg Response Element (WRE) responsible for cardiac expression of *even-skipped* (*eve*) is also directly regulated by Decapentaplegic (Dpp) and RAS signaling (Halfon et al., 2000; Knirr and Frasch, 2001; Han et al., 2002). A high degree of specificity is also observed in vertebrate cell culture, where microarray analysis revealed minimal overlap between Wnt targets in different cell types (Vlad et al., 2008).

Many developmental signaling pathways activate the expression of feedback antagonists, which limit their range of action. These include *naked cuticle (nkd)* and *notum/wingful* for Wg signaling (Gerlitz and Basler, 2002; Giraldez et al., 2002; Zeng et al., 2000), as well as *patched*, *daughters against dpp* and *argos* for the Hedgehog, Dpp and Epidermal Growth Factor signaling pathways, respectively (Alexandre et al., 1996; Golembo et al., 1996; Tsuneizumi et al., 1997). In contrast to the cell-specific nature of most target genes, these feedback antagonists are ubiquitously activated by their respective signaling pathways regardless of cell type. The regulatory cis-acting sequences controlling these universal responders have not been characterized. Do universal enhancers activate expression of these antagonists in all cell types, or do these targets require multiple tissue-specific enhancers? To address this question, we examined the regulation of *nkd* by Wg signaling.

nkd has all the essential features of a signal-induced feedback antagonist. Its expression requires Wg signaling and it is often expressed in a slightly broader pattern than Wg, owing to the ability of secreted Wg to diffuse to neighboring cells (Zeng et al., 2000). *nkd* encodes an EF hand protein that is thought to antagonize Wg signaling through binding to Dishevelled, a protein which mediates Wg-dependent stabilization of Arm (Rousset et al., 2001). Loss of *nkd* in fly embryos results in elevated Arm levels and ectopic activation of Wg signaling, causing a dramatic reprogramming of epidermal cell fate (Waldrop et al., 2006; Zeng et al., 2000).

Our lab previously identified a WRE in the first intron of the *nkd* gene that is bound by TCF and activated by Wg signaling in cell culture (Fang et al., 2006; Li et al., 2007; Parker et al., 2008). In this report, we used chromatin immunoprecipitation (ChIP) to identify a region upstream of the *nkd* gene that is also bound by TCF. This region contains two overlapping WREs (UpE1 and UpE2). Mutagenesis of TCF binding sites in these WREs and the intronic WRE (IntE) demonstrate direct regulation by the pathway through TCF. Each of these WREs is activated by Wg signaling in patterns very similar to that of *nkd* transcripts. The WREs are active in broad, partially overlapping patterns in larval imaginal discs, and the sum of the three can largely account for the entire *nkd* pattern in late third instar larva. In contrast, these WREs only partially recapitulate the embryonic *nkd* pattern. When deleted from the endogenous *nkd* locus, loss of IntE has a minimal effect on *nkd* expression whereas loss of a region containing UpE1/UpE2 displays a dramatic reduction in imaginal disc expression. However, neither deletion affected embryonic expression of *nkd*. Our data demonstrate that multiple WREs are needed for *nkd* to respond to Wg signaling in all tissues. The overlapping specificity

of these WREs may provide robustness to the Wg-Nkd feedback circuit in the various cells where it operates. In addition, multiple *nkd* WREs may have been required for the activation of *nkd* to be maintained as the expression of the Wg ligand became more elaborate during animal evolution.

Materials and Methods

Drosophila cell culture

Kc167 (Kc) and S2R+ cells were cultured in the Schneider's *Drosophila* media (Invitrogen) containing 5% or 10% FBS at 25°C, respectively. Clone8 cells were cultured as described (http://flyrnai.org/RNAi_index.html).

RNAi, Wg-conditioned media (Wg-CM) treatment and qRT-PCR

Double-stranded RNA (dsRNA) corresponding to *control*, *Axin*, *arm*, and *TCF* was synthesized as described (Fang et al., 2006). The Wg pathway in cultured cells was activated by depleting *Axin* or adding Wg-CM as described (Chang et al., 2008; Fang et al., 2006; Li et al., 2007). Briefly, 1×10^6 Kc, S2R+ or Clone 8 cells were seeded in 12-well plates and 10 ug of *Axin* or control dsRNA were added to each well. When *Axin* dsRNA was combined with another RNA duplex, 10 ug of each dsRNA was used. Cultures were incubated with dsRNAs for 6 days before harvesting for qRT-PCR analysis.

Wg-CM was prepared using stable p*Tub-wg* S2 cells, kindly provided by Dr Roel Nusse from Stanford University. Wg-CM was collected from dense cultures (typically 7–10 million cells/ml) lacking hygromycin. Usually 200 ul of unconcentrated Wg-CM was added to 600 ul cell suspensions containing 1–3 million cells. As a control, media collected from S2 cells was used. Cells were treated for 5 hours with control media or Wg-CM before harvesting for qRT-PCR analysis.

After the treated cells were collected, total RNA was isolated with Trizol reagent (Invitrogen) and cDNA synthesis was performed using Superscript III reverse transcriptase (Invitrogen) according to the manufacturer's protocols. Additional details of the qRT-PCR and the primer sequences used are described (Fang et al., 2006).

Chromatin immunoprecipitation (ChIP)

ChIP analysis was performed essentially as described (Fang et al., 2006) except that the dimethyl 3,30-dithio-bis(propionimidate) dihydrochloride treatment was eliminated. Typically 3×10^6 cells and 5–10 ul of TCF antibody were used per ChIP and all precipitated DNA samples were quantified by qPCR. Data are expressed as the percent of input DNA. The specific primer pairs for UpE, IntE and ORF correspond to #N1, #N5, and #N0 primer sets described previously (Fang et al., 2006).

Plasmids

Luciferase reporter constructs containing various *nkd* WREs were made by incorporating *Mlu*I/*Xma*I PCR fragments into a *pGL3-Basic* vector (Promega) containing the *Drosophila hsp 70* minimal promoter. *hsp 70* promoter was cloned into *pGL3-Basic* via PCR using 5' ATCTCGAGCTCGAGATCTGAGCGCCGGAGT3' (*Xho*I site is underlined) and 5'ATAAGCTTAAGCTTCCCAATTCCCTATTCAGAGTTCTC3' (*Hin*dIII site is underlined) primers. The specific primers to amplify the UpE and IntE genomic fragments are the following: UpE, 5'TCCTACGCGTGGCTGGGCTCGATGCAGATAA3' and 5'AATTCCCGGGGG CCGCTGTCGGCCAACTG3'; UpE1, 5'TCCTACGCGTGGCTGGGCTCGATGCAGA TAA3' and 5'GGTGCCCGGGTTTGTAGTTTGCGGTGGT3'; UpE2, 5'AATTACGCGTCAG

GAGGTCTGCCAACTTAAGTAG3' and 5'AATTCCCGGGGGGCCGCTGTCGGCCAAC TG3'; IntE (869 bp) 5'TTAGACGCGTGCTCTCGGGCCAC3' and 5'CCAGCCCGGG TTCCTCAAAGCAACC3'; IntE (255 bp) 5'GCCACGCGTATAGTTTGTGTATAGTT3' and 5'CCCAGCCCGGGTTCCTCAAAGCAACC3'. The *Mlu*I (ACGCGT) and *Xma*I sites (CCCGGG) are underlined. Deletions of the WREs (UpE #1, #2, #3, and IntE 558bp) were made by standard PCR cloning or subcloning.

TCF binding sites in the reporter constructs were destroyed using quick change site-directed mutagenesis (Stratagene). Base substitutions were A to C or T to G (or vice versa). For UpE1 and UpE2 all eight nucleotides of the TCF binding site (SSTTTGWW) were substituted while the 4th, 6th and 7th positions were altered in IntE.

For analysis in fly tissues, WREs were cloned into the pH-Pelican lacZ reporter (Barolo et al., 2000) and introduced into the fly genome by P-element transgenesis (Bestgene Inc.). The combined *nkd* WRE has a 1084 bp UpE fragment upstream of a 869 bp IntE fragment.

Transfection and reporter gene assays

Transient transfections and reporter assays were done essentially as previously described (Fang et al, 2006, Li et al., 2007). Briefly, a mixture of plasmids containing 100 ng luciferase reporter, 5 ng *pAclacZ* (Invitrogen) and 100 ng of *pAc-Arm** (Fang et al., 2006) were co-transfected with 1 × 10^6 cells. The *pAc-Arm** is a derivative of *pAc5.1* expression vector (Invitrogen) encoding a constitutively active form of Arm which has Thr^{52}, Ser^{56} substituted with Ala (Freeman and Bienz, 2001). The empty *pAc5.1* vector was used to normalize the DNA content or as controls. Cells were harvested 3 days after transfection for further reporter assays.

Luciferase and β-galactosidase activities were assayed using the Tropix Luc-Screen and Galacto-Star kits (Applied Biosystems) and quantified with a Chameleon plate luminometer (Hidex Personal Life Science). Transfection efficiency was normalized using the *pAclacZ* β-galactosidase activities. When Wg–CM was used to activate Wg signaling instead of co-expression of Arm*, cells were transfected with the same amount of reporter and *pAcLacZ* and incubated for 2 days before the cells were treated with Wg-CM for 24 h prior to harvesting for the reporter assays.

Drosophila genetics

Fly stocks were maintained on standard medium at 25°C unless otherwise indicated. The P [*En-Gal4*] and P[*Dpp-Gal4*] are as described (Li et al., 2007). The dominant negative *TCF* transgene (P[*UAS-TCF^{DN}*]) and constitutively active arm (P[*UAS-arm^{S10}*]) were obtained from M. Peifer (Pai et al., 1997; van de Wetering et al., 1997). *wg^{CX4}* is a molecular null (van den Heuvel et al., 1993). *Df(3L)ED4782*, a large (175 kb) deficiency lacking the entire *nkd* locus and a hypomorphic allele *nkd$^{l(3)4869}$* (Zeng et al., 2000) were obtained from Bloomington Stock Center. Homozygous *Df(3L)ED4782* embryos and *Df(3L)ED4782/nkd$^{l(3)4869}$* transheterozygotes display loss of cuticular denticles characteristic of *nkd* loss-of-function. Experiments with *En-Gal4 and Dpp-Gal4* were carried out at 25°C.

A 13 kb deletion lacking UpE (Δ*UpE*) was generated by mitotic recombination using *hsFLP* and *PBac{RB}e00194* and *P{XP}d09466* chromosomes (Parks et al., 2004). Two transposon insertions, *PBac{RB}e00194* and *P{XP}d09466* (obtained from the Exelixis stock center, Harvard Medical School) were outcrossed to *w^{1118}* flies for three generations before isogenization, removing at least one linked lethal from each line. In the dysgenic cross, males with darker eye color than any of single transposon line were obtained (see Supplemental Fig. 5) and molecular mapping with PCR confirmed the deletion. The Δ*UpE* allele is homozygous

semi-lethal but Δ*UpE/Df(3L)ED4782* transheterozygotes are viable and fertile. This indicates that the semi-lethality of homozygous Δ*UpE* is due to a linked mutation(s).

A 3 kb genomic deletion removing IntE was created by imprecise excision of the *P*[*KG0529*] transposon (obtained from Bloomington Stock Center) as described previously (Zhou et al., 2003). The *P*[*KG0529*] line was outcrossed to w^{1118} flies for three generations before isogenization. The deletion was characterized using PCR and the relevant PCR bands were sequenced to confirm the deletion breakpoints.

Immunostaining, in situ hybridization and microscopy

Immunostaining and *in situ* hybridization of fly embryos and imaginal discs were performed as described previously (Lin et al., 2004; Parker et al., 2002), using rabbit anti-LacZ (1:500) (Abcam Inc.), guinea-pig anti-Sens (1:500) (Fang et al., 2006) and mouse anti-Wg antisera (1:100) (Developmental Studies Hybridoma Bank at the University of Iowa). Cy3- and Alexa 488-conjugated secondary antibodies were from Jackson Immunochemicals and Molecular Probes, respectively. Samples were examined using Leica confocal microscope DM6000B-CS (Leica) and processed in Adobe Photoshop 8.0.

Probes for *in situ* hybridization of *nkd* transcripts were made by PCR of genomic DNA with the following oligos: 5'GAATTAATACGACTCACTATAGGGAGAGCTGCTGGTC AGCGAACGTGACAATAA3' and 5'GAATTAATACGACTCACTATAGGGAGACAGACC CGTGGGCAACTTCTTCAGTTT3'. Underlined sequences are T7 promoter sites. Antisense dioxygenin probes were synthesized using the Ambion T7 Megascript kit with the Roche DIG RNA labeling mix. Samples for *in situ* analysis were photographed with a Nikon Eclipse800 compound microscope using DIC optics.

Quantification of nkd transcripts in wing imaginal discs

20 wing imaginal discs were collected from late 3rd instars of transheterozygotes *+/Df(3L) ED4782*, Δ*UpE/Df(3L)ED4782*, and Δ*IntE/Df(3L)ED4782* flies. After pelleting, the discs were homogenized with 1.5 pellet pestles (South Jersey Precision Tool and Mold Inc.) in 200 µl Trizol reagent (Invitrogen). After addition of another 300 µl of Trizol, the samples were processed according to the manufacturer's protocols. Total RNA was resuspended in 10 ul of RNAase-free water and 2 ug of total RNA was used to synthesize cDNA using Superscript III (Invitrogen) according to the manufacturer's protocol. *nkd* and β-*tubulin 56B* transcripts were measured by qRT-PCR with primers used for cell culture experiments (Fang et al., 2006). The level of *nkd* transcript was normalized by the level of β-*tubulin 56B*. The value for *nkd* transcripts from *+/Df(3L)ED4782* flies was normalized to 1 and the relative level of transcripts in Δ*UpE or ΔIntE* was determined. The error represents the standard deviations from four independent experiments.

Results

The nkd locus contains several WREs that are directly activated by Wg signaling in cultured cells

As previously reported (Fang et al., 2006; Li et al., 2007; Parker et al., 2008), expression of *nkd* is induced in *Drosophila* Kc167 (Kc) cells upon stimulation with Wg-conditioned media (Wg-CM) or RNAi depletion of *Axin*. RNAi knockdown of either *TCF* or *arm* significantly reduced this *nkd* induction (Fig. 1A, B). When the *nkd* transcription unit and surrounding DNA (see cartoon in Fig. 1C) were assayed for TCF binding via ChIP, TCF was highly enriched in the region containing an intronic WRE (IntE) and this binding was enhanced upon Wg-CM

treatment (Fang et al., 2006; Parker et al., 2008). Thus, IntE is likely to be a major WRE in mediating Wg-dependent activation of *nkd* expression in Kc cells.

Occasionally, more modest TCF binding was also observed ~10 kb upstream of the *nkd* transcriptional start site (TSS) in Wg-CM treated Kc cells (Parker et al., 2008). TCF binding to this upstream region (UpE) was much more pronounced when cells were treated with *Axin* RNAi, reaching levels similar to those seen at IntE (Fig. 1D). Cells simultaneously depleted for Axin and TCF lost TCF binding at both locations, demonstrating the specificity of the TCF antisera (Fig. 1D). As observed previously (Fang et al., 2006; Li et al., 2007; Parker et al., 2008), no significant binding of TCF was found at the ORF (Fig. 1D).

To test whether UpE is a functional WRE, a genomic fragment (1084 bp) containing this region was cloned into a *hsp 70* core promoter/luciferase reporter. Such reporters can be assayed for Wg responsiveness by cotransfection with a stabilized form of Arm (Arm*) (Fang et al., 2006; Parker et al., 2008). This UpE fragment was activated almost 1000-fold by co-expression with Arm* (Fig. 2A), indicating that it possesses a high level of WRE activity.

To further localize the WRE activity in UpE, it was split into three parts and tested in reporter assays. None of the smaller fragments (#1, #2 or #3) had high WRE activity (Fig. 2A). However, regions containing the 5' (UpE1) or 3' (UpE2) two thirds of UpE were dramatically activated by Arm* (Fig. 2A). These data suggest that the UpE region contains two WREs, albeit with overlapping sequences.

UpE1, UpE2 and IntE all contain multiple predicted TCF binding sites (Fig. 2) that are conserved among the sequenced *Drosophila* species, including the distantly related *D. virilis* (Supplemental Fig. 1B, C). Examination of the nine conserved TCF sites reveals a consensus of SCTTTGW (S = G or C; W = A or T) very similar to the preferred binding site of fly TCF (CCTTTGAT) (van de Wetering et al., 1997). In the 869 bp IntE previously identified (Fang et al., 2006), all three sites are clustered at the 3' end of the fragment (Fig. 2B). A 255 bp fragment containing all three TCF sites still possessed a high level of WRE activity, though less than that of the 869 bp fragment (Fig. 2B).

To determine whether the conserved TCF sites in these WREs are functional, they were destroyed by site-directed mutagenesis. Individual mutation of the five TCF sites in UpE2 demonstrated that three of the five contributed to WRE activity (Supplemental Fig. 2A). Individual mutations in any of the three TCF sites in IntE (255 bp) reduced WRE activity (Supplemental Fig. 2B). Simultaneous mutation of three TCF sites in UpE1 resulted in a large reduction in Wg responsiveness (Fig. 2A). More emphatically, mutation of two TCF sites in UpE2 or all three sites in IntE completely abolished the activity of these WREs (Fig. 2A, B). Together with the ChIP data, the mutagenesis results demonstrate that these WREs are directly activated by TCF-Arm in Kc cells.

UpE1, UpE2 and IntE are highly responsive to Arm* in Kc cells (Fig. 2), which are derived from embryonic hemocytes (Goto et al., 2001). These WREs are also activated by Arm* in two other fly cell lines, S2R+ and Clone8 (Supplemental Table 1), derived from embryonic hemocytes and wing imaginal disc epithelia cells, respectively (Peel et al., 1990;Yanagawa et al., 1998). In addition, these WREs were also highly activated by Wg-CM treatment (Supplemental Table 1).

The TCF binding and reporter gene data suggest that the UpE1 and UpE2 act as WREs for the *nkd* locus but it is also possible that they activate other nearby genes. To explore this, three genes that are upstream of the *nkd* TSS (*mkp3*, *CG3797* and *Acp76A*) and two downstream of the 3' end of the gene (*CG18136* and *CG3808*) were tested for Wg responsiveness. The only gene whose expression was altered by *Axin* RNAi was *CG3808*, which showed a 1.8 fold

increase (*nkd* was activated 56 fold in the same experiment; data not shown). This suggests that UpE1 and UpE2 mediate transcriptional activation of the *nkd* gene by Wg signaling.

The nkd-WREs identified from cultured cells are also directly activated in vivo by Wg signaling

Wg is expressed in many embryonic tissues (e.g., Fig. 3A, F) and larval imaginal discs (e.g., Fig. 3K, P, U). In all tissues examined, *nkd* transcripts are found in patterns similar to that of Wg (e.g., Fig. 3E, J, O, T, Y). In some tissues the *nkd* pattern is broader than that of Wg (compare Fig. 3A and U with Fig. 3E and Y), consistent with non-autonomous activation by the secreted Wg ligand (Zeng et al., 2000).

To determine whether the WREs from the *nkd* locus reflect the endogenous *nkd* pattern in fly tissues, *nkd*-UpE1, UpE2 and IntE (the 869 bp fragment) were cloned into the pH-Pelican lacZ reporter (Barolo et al., 2000) and introduced into the fly genome by P element transgenesis. All three reporters were expressed in patterns reminiscent of *nkd* transcript distribution. UpE1 was active in multiple imaginal discs (Fig. 3L, Q, V) but displayed no activity during embryogenesis (Fig. 3B, G). UpE2 partially recapitulates the epidermal striped *nkd* pattern during germband extension (Fig. 3C) but was not expressed in older embryos (Fig. 3H). UpE2 also has activity in several imaginal discs (Fig. 3M, R, W). IntE did not express LacZ reporter at germband extension (Fig. 3D), but was active in the mesoderm and endoderm in older embryos (Fig. 3I). This reporter also displayed activity in late third instar imaginal discs (Fig. 3N, S, X). In summary, each reporter recapitulated part of the endogenous *nkd* pattern.

The expression patterns of the *nkd*-WREs in various fly tissues are summarized in Table 1. In the larval eye disc, the activities of all three reporters are very similar (Fig. 3V–X). However, in all other tissues the WREs display a fair degree of specificity. While all three WREs were active in the leg discs, UpE1 activation was largely restricted to the columnar epithelia of the disc (Fig. 3Q) while IntE was mostly active in the peripodial membrane (Fig. 3S). UpE2 was active in both cell types (Fig. 3R). In the wing pouch, hinge region and antennae primordia, UpE1 and UpE2 are active (though UpE2 is significantly stronger) while IntE is very weak or not detected (Fig. 3L–N, V–X). Conversely, in older embryos, IntE is active in several mesodermal and endodermal tissues (Fig. 3I) similar to *nkd* (Fig. 3J) but UpE1 and UpE2 have no activity (Fig. 3G, H). In the notum, UpE1 is most active (Fig. 3L), IntE has intermediate expression (Fig. 3N) while UpE2 is not active (Fig. 3M). These data demonstrate that these WREs have partially overlapping patterns, but that they are also selectively used in many tissues.

All the lacZ expression patterns described for the *nkd*-WREs are consistent with activation by Wg signaling. In several cases this was demonstrated experimentally. When the IntE reporter was crossed into a *wg* null mutant background, the expression pattern was lost in several tissues (compare Fig. 4B with 4A), except for the activity at the leading edge of the migrating dorsal epithelia (arrow in Fig. 4B). Wg regulation of these reporters in the wing imaginal disc was tested by expressing a dominant-negative form of *TCF* (TCF^{DN}) in the posterior part of the wing pouch, via *en-Gal4*. TCF^{DN} is known to potently inhibit Wg signaling (van de Wetering et al., 1997), as exemplified by inhibition of Sens (arrowheads in Fig. 4L; compare to Fig. 4K), a known Wg target (Parker et al., 2002). UpE1 and UpE2 expression was markedly reduced by TCF^{DN} (arrowheads in Fig. 4F and 4I). Conversely, expression of an active form of *Arm* (Arm^{S10}) (Pai et al., 1997) via *dpp-Gal4* caused a dramatic increase in UpE1 expression in the wing pouch (arrows in Fig. 4G). Similar activation by Arm^{S10} was observed for UpE2 and IntE (data not shown). In all cases examined, loss of Wg signaling dramatically reduced *nkd*-WRE activity while activation of the pathway increased reporter expression.

To demonstrate that UpE2 and IntE are directly regulated by TCF in fly tissues, the functional TCF sites identified in cell culture (Fig. 2A, B) were destroyed in the WRE-lacZ reporters. In the case of IntE, a shorter (255 bp) transgene was the starting point. IntE (255 bp) has an identical pattern to the longer IntE (869 bp) but the expression is less robust in most tissues (Fig. 4C and data not shown). Mutation of the three TCF sites in IntE (255 bp) abolished the expression of LacZ in stage 13 embryos (Fig. 4D) and various imaginal discs (data not shown). In the case of UpE2, altering two TCF sites drastically reduced lacZ expression in the wing disc (Fig. 4J) and all other imaginal discs examined (data not shown). Thus, IntE and UpE2 are directly activated by Wg signaling in several fly tissues.

UpE and IntE are not sufficient to recapitulate the embryonic nkd pattern

The patterns of UpE1, UpE2 and IntE appear to cover most of the endogenous *nkd* pattern in the imaginal discs of late third instar larva. However, the sum of these WREs accounts for only part of the endogenous embryonic pattern of *nkd* (Fig. 3). To test whether the UpE region and IntE might act synergistically in the embryo, transgenic animals containing the entire UpE (1084 bp) and IntE (869 bp) cloned into the pH-Pelican vector (Fig. 5A) were created and monitored for lacZ expression.

In the wing imaginal discs, the combined WRE reporter was active in all the locations observed with the individual UpE1, UpE2 and IntE reporters (Fig. 5B). However, the pattern was slightly more than the sum of the three individual WREs. For example, the combined reporter had elevated lacZ expression on either side of the Wg stripe at the dorsal/ventral boundary (Fig. 5B). In addition, the level of expression in the wing pouch and hinge region was consistently elevated in the combined reporter. Because of the elevated lacZ expression in this portion of the wing disc, the expression in the notum appears weaker in the combined reporter compared to the UpE1 reporter (compare Fig. 5B to Fig 3L). However, the level of expression of both reporters in the notum appear roughly similar (data not shown). The expression of the combined WRE reporter in the eye/antennal and leg imaginal discs is similar to that of endogenous *nkd* and appears to be the sum of the three individual WRE reporters (data not shown).

In embryos, the combined WRE reporter was active in weak stripes at germband extension (Fig. 5C), a pattern similar to UpE2 (Fig. 3C). In older embryos, the pattern of the combined WRE reporter (Fig. 5D) was similar to that found in IntE embryos (Fig. 3I). The additive nature of the expression patterns indicates no detectable cooperative interactions between UpE and IntE, suggesting that at least one other WRE exists in the *nkd* locus which might account for the missing embryonic pattern.

The data obtained from reporter assays strongly support the model that UpE1, UpE2 and IntE are bona fide WREs of *nkd*. To determine whether UpE or IntE were required for expression of endogenous *nkd*, two deletions in the gene were created. Using transposons inserted in the locus that contain Flp recombinase recognition sites (FRTs) (Parks et al., 2004), a deletion removing approximately 13 kb of sequence upstream of the *nkd* TSS (Δ*UpE*; Fig. 6A) was engineered (see Materials and Methods and Supplemental Fig. 3 for more details). Imprecise excision of a P-element in IntE was used to generate the Δ*IntE* allele, which lacks approximately 3 kb of intronic sequence including IntE (Fig. 6B).

To test the effect of the Δ*UpE* and Δ*IntE* alleles on *nkd* expression, they were placed over *Df (3L)ED4782*, a large (175 kb) deficiency removing *nkd* and several surrounding genes. These transheterozygous backgrounds produced viable fertile adults at about the same frequency as *+/Df(3L)ED4782* individuals (data not shown). Since mutations in the *nkd* gene are embryonic lethal (Zeng et al., 2000), the viability of Δ*UpE/Df(3L)ED4782* and Δ*IntE/Df(3L)ED4782* indicates that UpE and IntE are dispensable for *nkd* expression in the embryo. Consistent with

this, no detectable reduction in *nkd* transcript level was detected from Δ*UpE/Df(3L)ED4782* and Δ*IntE/Df(3L)ED4782* embryos as judged by *in situ* hybridization (data not shown).

Unlike the situation in the embryo, Δ*UpE* did affect *nkd* expression in larval tissues. *In situ* hybridization revealed that Δ*UpE/Df(3L)ED4782* larvae had a marked reduction in *nkd* transcript levels compared to *+/Df(3L)ED4782* controls in the wing and leg imaginal discs (Fig. 6C, D, F, G). A similar reduction was observed in the eye-antennal discs (data not shown). qRT-PCR quantification revealed that Δ*UpE/Df(3L)ED4782* wing discs had 41% (S.D. ± 26%) of the *nkd* mRNA found in control wing discs. In contrast to Δ*UpE*, loss of IntE did not detectably change *nkd* expression in the imaginal discs, as judged by *in situ* hybridization (Fig. 6E, H) and qRT-PCR of RNA from wing imaginal discs (data not shown). With the important caveat that the Δ*UpE* allele deletes almost 12 kb of sequence besides UpE, the data obtained are consistent with the idea that UpE is a bona fide WRE of *nkd*. IntE, on the other hand is dispensable for expression of endogenous *nkd* in the tissues that were examined.

Discussion

We previously identified binding of TCF to a region in the *nkd* intron that corresponds to IntE (Fang et al., 2006; Parker et al., 2008). In this report, we find that TCF is also highly enriched on the chromatin about 10 kb upstream of the *nkd* TSS (UpE) when the Wg pathway is chronically activated by *Axin* RNAi (Fig. 1). Wg signaling also increases the binding of TCF to the region containing IntE (Fig. 1), but this effect occurs within a few hours of pathway stimulation (Fang et al., 2006; Parker et al., 2008). The increase in TCF-binding in the UpE region is not due to increased TCF, since the expression of TCF and its nuclear localization are not affected by *Axin* RNAi (Chang et al., 2008). Rather, we postulate that widespread histone acetylation at the *nkd* locus upon Wg stimulation (Parker et al., 2008) allows subsequent recruitment of TCF to the UpE region in Kc cells.

Further analysis of the UpE region with reporter gene assays revealed the presence of two overlapping stretches of DNA (UpE1 and UpE2) that confer a high degree of responsiveness to Wg signaling (Fig. 2A). Mutagenesis of two to three predicted TCF binding sites in UpE1, UpE2 and IntE largely abolished their ability to respond to Wg signaling (Fig. 2A,B). While this suggests that TCF sites within a WRE act in a redundant manner, mutation of individual sites indicates that some sites contribute more than others. For example, in UpE2, the TCF 2 and TCF 3 sites share the same sequence (Supplemental Fig. 1A), but mutation of TCF 2 reduces Wg activation while mutation of TCF 3 does not (Supplemental Fig. 2A). These data suggests that the exact sequence of the TCF binding site is likely not as important as the context in which they are located within the WRE.

When tested in flies, UpE1, UpE2 and IntE are all activated by Wg signaling in several tissues in patterns that partially recapitulate that of the endogenous *nkd* gene (Fig. 3, Fig. 4 & Table 1). In the leg and eye imaginal discs, all three WREs are active. In addition, each WRE has unique tissue-specific activities. For example, in later embryogenesis IntE is the only WRE that is active. Even though UpE1 and UpE2 share more than 400 bp of sequence (Fig. 2A), only UpE2 is active in the embryonic epidermis. UpE1 and UpE2 are both active in the wing and antennal imaginal discs, (IntE shows no or minimal expression in these tissues), but UpE1 is expressed strongly in the notum whereas UpE2 is not. Each WRE is active in multiple tissues but also contains information that confers tissue-specific Wg responsiveness.

The basis for the tissue specificity of the various *nkd*-WREs is not clear at present. It could be that different TCF sites within each WRE are utilized in different tissues. However, our data in cell culture argue that multiple TCF sites are required in each WRE in a partially redundant manner (Fig. 2; Supplemental Fig. 2). In addition, the same TCF sites that are required for

UpE2 and IntE activity in Kc cells are required for WRE activation in all tissues examined (Fig. 4D, J; data not shown). Therefore, we favor the view that the tissue specificity for the different WREs is derived from the presence of other cis-acting elements that work with the TCF sites to allow activation by Wg signaling.

When all three WREs are placed within a single reporter construct the resulting pattern largely recapitulates that of the endogenous *nkd* gene in imaginal discs at the late third larval instar stage (Fig. 5B; data not shown). However, we have not examined the regulation of our WRE reporters at earlier larval stages, where Wg is also expressed (Williams et al., 1993;Neumann and Cohen, 1996). Even at the late larval stage examined, the pattern of the reporters does not completely match that of endogenous *nkd* in the wing disc. Wg is expressed in a double ring pattern in the hinge region (Fig. 3K; the proximal ring indicated by the arrow) and *nkd* transcripts are also found in a double ring (Fig. 6C; arrow). However, expression of WRE reporters in the proximal ring is weak (Fig. 3M) and often not present (Fig. 5B). This suggests the existence of at least one other WRE for the wing imaginal disc.

In the embryo, it is even more obvious that additional regulatory information for *nkd* expression remains to be identified. In the embryonic epidermis the pattern of the combined WRE construct is only a subset of the endogenous *nkd* pattern and is equal to the sum of the IntE and UpE2 WREs (Fig. 5C, D; data not shown). This suggests the presence of at least one other WRE that is active in the embryonic epidermis. Consistent with this, deletions of genomic fragments containing IntE or UpE do not affect the expression of *nkd* in embryos or the viability of the animals when heterozygous with a *nkd* deficiency (data not shown).

In the wing and leg imaginal discs, loss of UpE results in a significant decrease in *nkd* transcript levels (Fig. 6D, G). In contrast, the IntE deletion had *nkd* expression in the normal range (Fig. 6E, H). Even with the large UpE deletion, there is still significant *nkd* expression in the wing disc (41% of wild type; see Results). These data could be evidence for redundancy between IntE and UpE in these tissues. It is also possible that additional WREs exist that contribute to imaginal disc expression, which are still present in the IntE and UpE deletions.

Our data indicate that *nkd* does not contain a universally responding WRE that is activated by Wg signaling in all tissues. Rather there are at least several WREs that can respond to the pathway in multiple, overlapping tissues. It appears that only limited multi-tissue responsiveness can be obtained with any individual WRE. In the absence of a universal WRE, the strategy of having multiple WREs responding to Wg signaling in each tissue may be required to ensure the robustness of the Wg-Nkd feedback circuit. Whether this is the case for the regulation of other Wnt feedback antagonists or those acting in other signaling pathways remains to be determined.

The finding that the *nkd* locus does not contain a universal WRE raises the question of how the Wg-Nkd relationship could remain intact during animal evolution as the Wg expression pattern became more elaborate. We postulate that the existence of several WREs with broad tissue specificity could have ensured that when an enhancer evolved that expressed Wg in a new location, at least one of the existing *nkd* WREs would be able to respond to the pathway in that tissue. This precludes the need to have a tissue-by-tissue *de novo* synthesis of *nkd* WREs every time Wg was expressed in a new pattern. Retaining the feedback inhibition of Wg signaling by Nkd may have allowed Wg to be used more readily during the diversification of animal body plans.

Supplementary Material

Refer to Web version on PubMed Central for supplementary material.

Acknowledgments

We thank members of the Cadigan lab for helpful discussions and Chandan Bhambhani in particular for careful reading of the manuscript. This work was supported by NIH Grant R01CA95869 to K.M.C.

References

Alexandre C, Jacinto A, Ingham PW. Transcriptional activation of hedgehog target genes in Drosophila is mediated directly by the cubitus interruptus protein, a member of the GLI family of zinc finger DNA-binding proteins. Genes Dev 1996;10:2003–2013. [PubMed: 8769644]

Barolo S, Carver LA, Posakony JW. GFP and beta-galactosidase transformation vectors for promoter/enhancer analysis in Drosophila. Biotechniques 2000;29:726–732. [PubMed: 11056799]

Bilder D, Scott MP. Hedgehog and wingless induce metameric pattern in the Drosophila visceral mesoderm. Dev. Biol 1998;201:43–56. [PubMed: 9733572]

Cadigan KM. Regulating morphogen gradients in the Drosophila wing. Semin. Cell Dev.Biol 2002;13:83–90.

Chang JL, Lin HV, Blauwkamp TA, Cadigan KM. Spenito and Split ends act redundantly to promote Wingless signaling. Dev. Biol 2008;314:100–111. [PubMed: 18174108]

Costas J, Pereira PS, Vieira CP, Pinho S, Vieira J, Casares F. Dynamics and function of intron sequences of the wingless gene during the evolution of the Drosophila genus. Evol. Dev 2004;6:325–335. [PubMed: 15330865]

Couso JP, Bate M, Martinez-Arias A. A wingless-dependent polar coordinate system in Drosophila imaginal discs. Science 1993;259:484–489. [PubMed: 8424170]

Fang M, Li J, Blauwkamp T, Bhambhani C, Campbell N, Cadigan KM. C-terminal-binding protein directly activates and represses Wnt transcriptional targets in Drosophila. Embo J 2006;25:2735–2745. [PubMed: 16710294]

Freeman M, Bienz M. EGF receptor/Rolled MAP kinase signalling protects cells against activated Armadillo in the Drosophila eye. EMBO Rep 2001;2:157–162. [PubMed: 11258709]

Gerlitz O, Basler K. Wingful, an extracellular feedback inhibitor of Wingless. Genes Dev 2002;16:1055–1059. [PubMed: 12000788]

Giraldez AJ, Copley RR, Cohen SM. HSPG modification by the secreted enzyme Notum shapes the Wingless morphogen gradient. Dev. Cell 2002;2:667–676. [PubMed: 12015973]

Golembo M, Schweitzer R, Freeman M, Shilo BZ. Argos transcription is induced by the Drosophila EGF receptor pathway to form an inhibitory feedback loop. Development 1996;122:223–230. [PubMed: 8565833]

Goto A, Kumagai T, Kumagai C, Hirose J, Narita H, Mori H, Kadowaki T, Beck K, Kitagawa Y. A Drosophila haemocyte-specific protein, hemolectin, similar to human von Willebrand factor. Biochem J 2001;359:99–108. [PubMed: 11563973]

Halfon MS, Carmena A, Gisselbrecht S, Sackerson CM, Jimenez F, Baylies MK, Michelson AM. Ras pathway specificity is determined by the integration of multiple signal-activated and tissue-restricted transcription factors. Cell 2000;103:63–74. [PubMed: 11051548]

Han Z, Fujioka M, Su M, Liu M, Jaynes JB, Bodmer R. Transcriptional integration of competence modulated by mutual repression generates cell-type specificity within the cardiogenic mesoderm. Dev. Biol 2002;252:225–240. [PubMed: 12482712]

Klingensmith J, Nusse R. Signaling by wingless in Drosophila. Dev. Biol 1994;166:396–414. [PubMed: 7813765]

Knirr S, Frasch M. Molecular integration of inductive and mesoderm-intrinsic inputs governs even-skipped enhancer activity in a subset of pericardial and dorsal muscle progenitors. Dev. Biol 2001;238:13–26. [PubMed: 11783990]

Lessing D, Nusse R. Expression of wingless in the Drosophila embryo: a conserved cis-acting element lacking conserved Ci-binding sites is required for patched-mediated repression. Development 1998;125:1469–1476. [PubMed: 9502727]

Li J, Sutter C, Parker DS, Blauwkamp T, Fang M, Cadigan KM. CBP/p300 are bimodal regulators of Wnt signaling. Embo J 2007;26:2284–2294. [PubMed: 17410209]

Lin HV, Rogulja A, Cadigan KM. Wingless eliminates ommatidia from the edge of the developing eye through activation of apoptosis. Development 2004;131:2409–2418. [PubMed: 15128670]

Neumann CJ, Cohen SM. Sternopleural is a regulatory mutation of wingless with both dominant and recessive effects on larval development of Drosophila melanogaster. Genetics 1996;142:1147–1155. [PubMed: 8846894]

Pai LM, Orsulic S, Bejsovec A, Peifer M. Negative regulation of Armadillo, a Wingless effector in Drosophila. Development 1997;124:2255–2266. [PubMed: 9187151]

Parker, DS.; Blauwkamp, T.; Cadigan, KM. Wnt/□-catenin-mediated transcriptional regulation. In: Sokol, S.; Wassarman, PM., editors. Wnt Signaling in Embryonic Development, Advances in Developmental Biology. Vol. Vol. 17. San Diego: Elsevier; 2007. p. 1-61.

Parker DS, Jemison J, Cadigan KM. Pygopus, a nuclear PHD-finger protein required for Wingless signaling in Drosophila. Development 2002;129:2565–2576. [PubMed: 12015286]

Parker DS, Ni YY, Chang JL, Li J, Cadigan KM. Wingless signaling induces widespread chromatin remodeling of target loci. Mol. Cell. Biol 2008;28:1815–1828. [PubMed: 18160704]

Parks AL, Cook KR, Belvin M, Dompe NA, Fawcett R, Huppert K, Tan LR, Winter CG, Bogart KP, Deal JE, Deal-Herr ME, Grant D, Marcinko M, Miyazaki WY, Robertson S, Shaw KJ, Tabios M, Vysotskaia V, Zhao L, Andrade RS, Edgar KA, Howie E, Killpack K, Milash B, Norton A, Thao D, Whittaker K, Winner MA, Friedman L, Margolis J, Singer MA, Kopczynski C, Curtis D, Kaufman TC, Plowman GD, Duyk G, Francis-Lang HL. Systematic generation of high-resolution deletion coverage of the Drosophila melanogaster genome. Nat. Genet 2004;36:288–292. [PubMed: 14981519]

Peel DJ, Johnson SA, Milner MJ. The ultrastructure of imaginal disc cells in primary cultures and during cell aggregation in continuous cell lines. Tissue Cell 1990;22:749–758. [PubMed: 2126897]

Pereira PS, Pinho S, Johnson K, Couso JP, Casares F. A 3' cis-regulatory region controls wingless expression in the Drosophila eye and leg primordia. Dev. Dyn 2006;235:225–234. [PubMed: 16261625]

Riese J, Yu X, Munnerlyn A, Eresh S, Hsu SC, Grosschedl R, Bienz M. LEF-1, a nuclear factor coordinating signaling inputs from wingless and decapentaplegic. Cell 1997;88:777–787. [PubMed: 9118221]

Rousset R, Mack JA, Wharton KA Jr, Axelrod JD, Cadigan KM, Fish MP, Nusse R, Scott MP. Naked cuticle targets dishevelled to antagonize Wnt signal transduction. Genes Dev 2001;15:658–671. [PubMed: 11274052]

Sanson B. Generating patterns from fields of cells. Examples from Drosophila segmentation. EMBO Rep 2001;2:1083–1088. [PubMed: 11743020]

Stadeli R, Hoffmans R, Basler K. Transcription under the control of nuclear Arm/beta-catenin. Curr. Biol 2006;16:R378–R385. [PubMed: 16713950]

Tsuneizumi K, Nakayama T, Kamoshida Y, Kornberg TB, Christian JL, Tabata T. Daughters against dpp modulates dpp organizing activity in Drosophila wing development. Nature 1997;389:627–631. [PubMed: 9335506]

van de Wetering M, Cavallo R, Dooijes D, van Beest M, van Es J, Loureiro J, Ypma A, Hursh D, Jones T, Bejsovec A, Peifer M, Mortin M, Clevers H. Armadillo coactivates transcription driven by the product of the Drosophila segment polarity gene dTCF. Cell 1997;88:789–799. [PubMed: 9118222]

van den Heuvel M, Harryman-Samos C, Klingensmith J, Perrimon N, Nusse R. Mutations in the segment polarity genes wingless and porcupine impair secretion of the wingless protein. Embo J 1993;12:5293–5302. [PubMed: 8262072]

Vlad A, Rohrs S, Klein-Hitpass L, Muller O. The first five years of the Wnt targetome. Cell Signal 2008;20:795–802. [PubMed: 18160255]

Waldrop S, Chan CC, Cagatay T, Zhang S, Rousset R, Mack J, Zeng W, Fish M, Zhang M, Amanai M, Wharton KA Jr. An unconventional nuclear localization motif is crucial for function of the Drosophila Wnt/wingless antagonist Naked cuticle. Genetics 2006;174:331–348. [PubMed: 16849595]

Williams JA, Paddock SB, Carroll SB. Pattern formation in a secondary field: a hierarchy of regulatory genes subdivides the developing Drosophila wing disc into discrete subregions. Development 1993;117:571–584. [PubMed: 8330528]

Yanagawa S, Lee JS, Ishimoto A. Identification and characterization of a novel line of Drosophila Schneider S2 cells that respond to wingless signaling. J. Biol. Chem 1998;273:32353–32359. [PubMed: 9822716]

Zeng W, Wharton KA Jr, Mack JA, Wang K, Gadbaw M, Suyama K, Klein PS, Scott MP. naked cuticle encodes an inducible antagonist of Wnt signalling. Nature 2000;403:789–795. [PubMed: 10693810]

Zhou H, Cadigan KM, Thiele DJ. A copper-regulated transporter required for copper acquisition, pigmentation, and specific stages of development in Drosophila melanogaster. J. Biol. Chem 2003;278:48210–48218. [PubMed: 12966081]

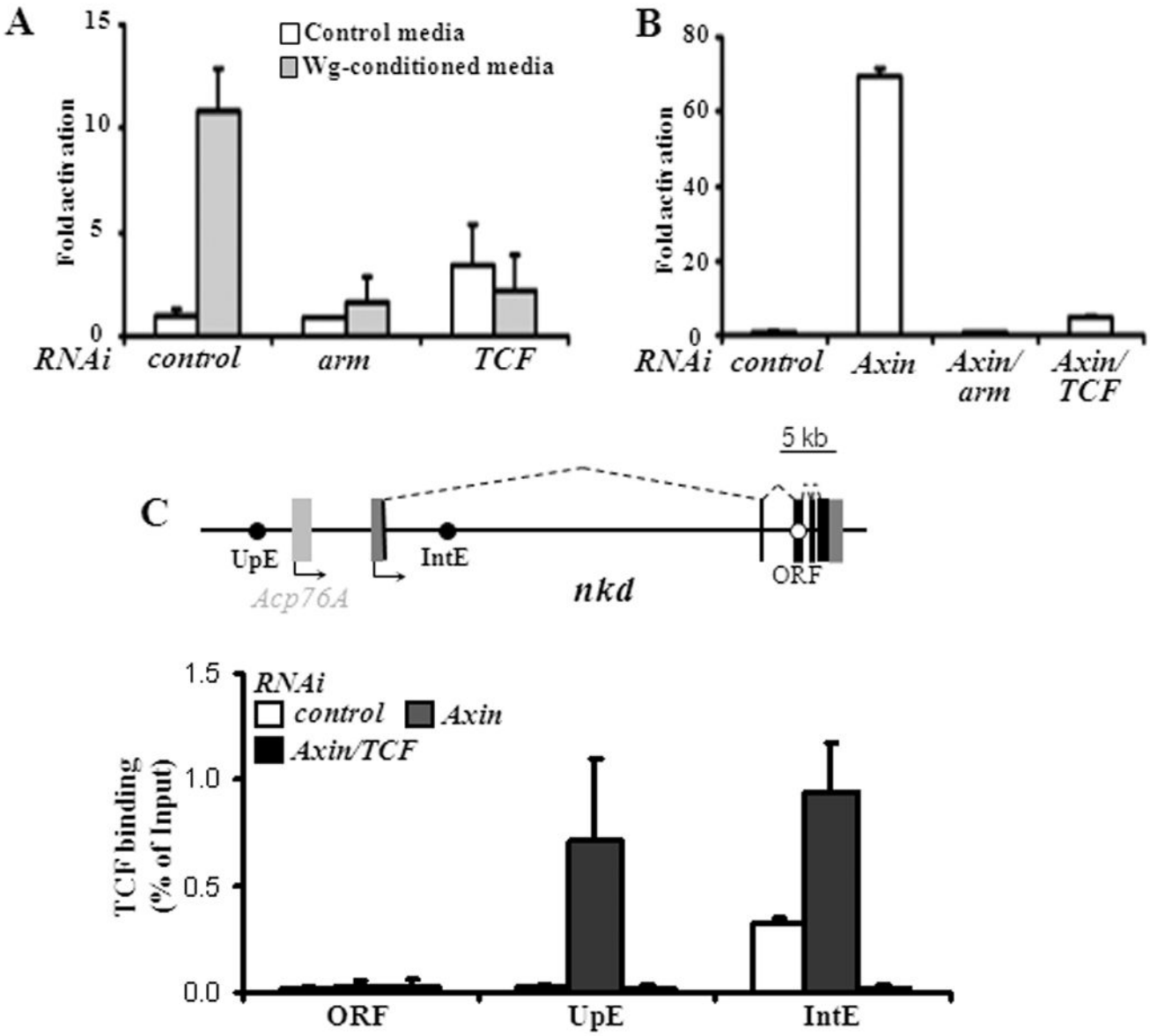

Fig. 1. TCF is recruited to two regions in or near the *nkd* transcription unit upon Wg stimulation of fly Kc cells

(A) Stimulation with Wg-CM for 5 hours resulted in elevated *nkd* expression, which was greatly reduced by RNAi depletion of *arm* or *TCF*. (B) Activation of Wg signaling by RNAi depletion of *Axin* for 6 days caused a huge increase in *nkd* transcript levels in an Arm and TCF-dependent manner. Transcript levels were determined by qRT-PCR as described in Materials and Methods. Fold activation is relative to *nkd* expression in cells treated with control RNAi and control media in panel A and control RNAi alone in panel B. Each bar is the mean of triplicates from cultures at each condition, with the standard deviation indicated. (C) Schematic of the *nkd* locus showing the location of three regions (UpE, IntE and ORF) assayed for TCF occupancy. *Acp76A* is not expressed at detectable levels in Kc cells. (D) Binding of TCF in Kc cells with the indicated RNAi treatments. In the absence of Wg signaling (*control* RNAi), TCF is bound to the region containing IntE but not UpE or ORF. In cells where the pathway is activated (*Axin* RNAi), there is strong binding to both UpE and IntE. TCF binding is

dramatically lowered in *Axin, TCF* depleted cells, indicating that the ChIP signal is specific for TCF. Each bar represents the mean of duplicate ChIP samples with the standard error indicated. The data shown are representative examples from more than three separate experiments.

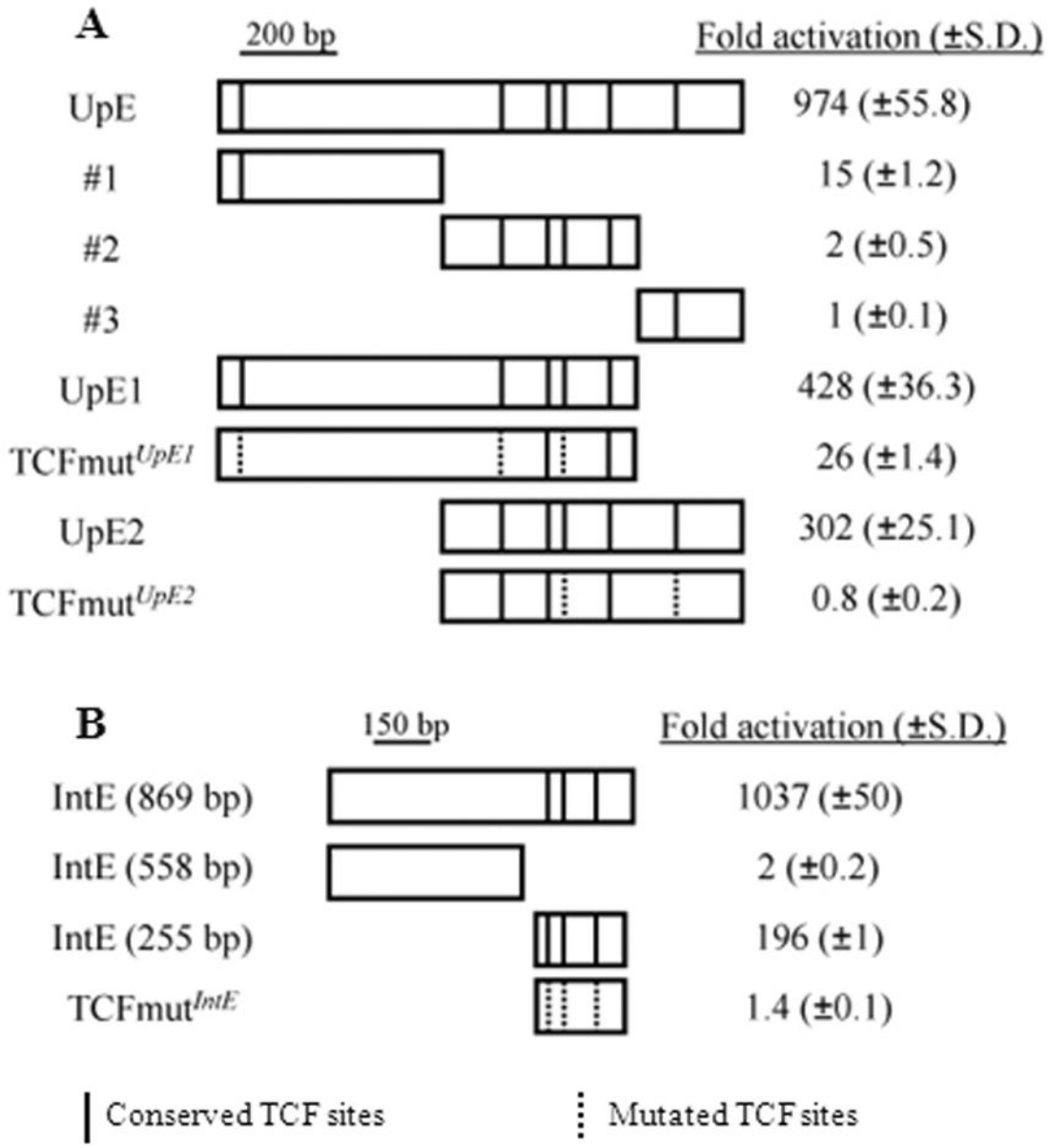

Fig. 2. Dissection of the UpE and IntE regions reveals WREs that contain functional TCF binding sites

(*A*) When cloned upstream of a *hsp70* core promoter/luciferase reporter, UpE activated luciferase expression when co-expressed with Arm*. UpE was divided into three fragments (#1 – 3), none of which were highly responsive to Arm*. However, two overlapping stretches (UpE1 and UpE2) possessed strong WRE activity. Vertical lines in the boxes represent the predicted TCF sites that are conserved in 12 *Drosophila* species, while the dotted lines denote mutated TCF sites. UpE1 and UpE2 both require a subset of the TCF sites for Arm* responsiveness. (*B*) The IntE genomic region contains a 255 bp WRE that requires three TCF binding sites for Arm* responsiveness. Fold activation is relative to luciferase expression without Arm* expression for each reporter construct. Each result is the mean of triplicate transfections, with the standard deviation indicated in parenthesis. The data shown are a representative example from more than three separate experiments.

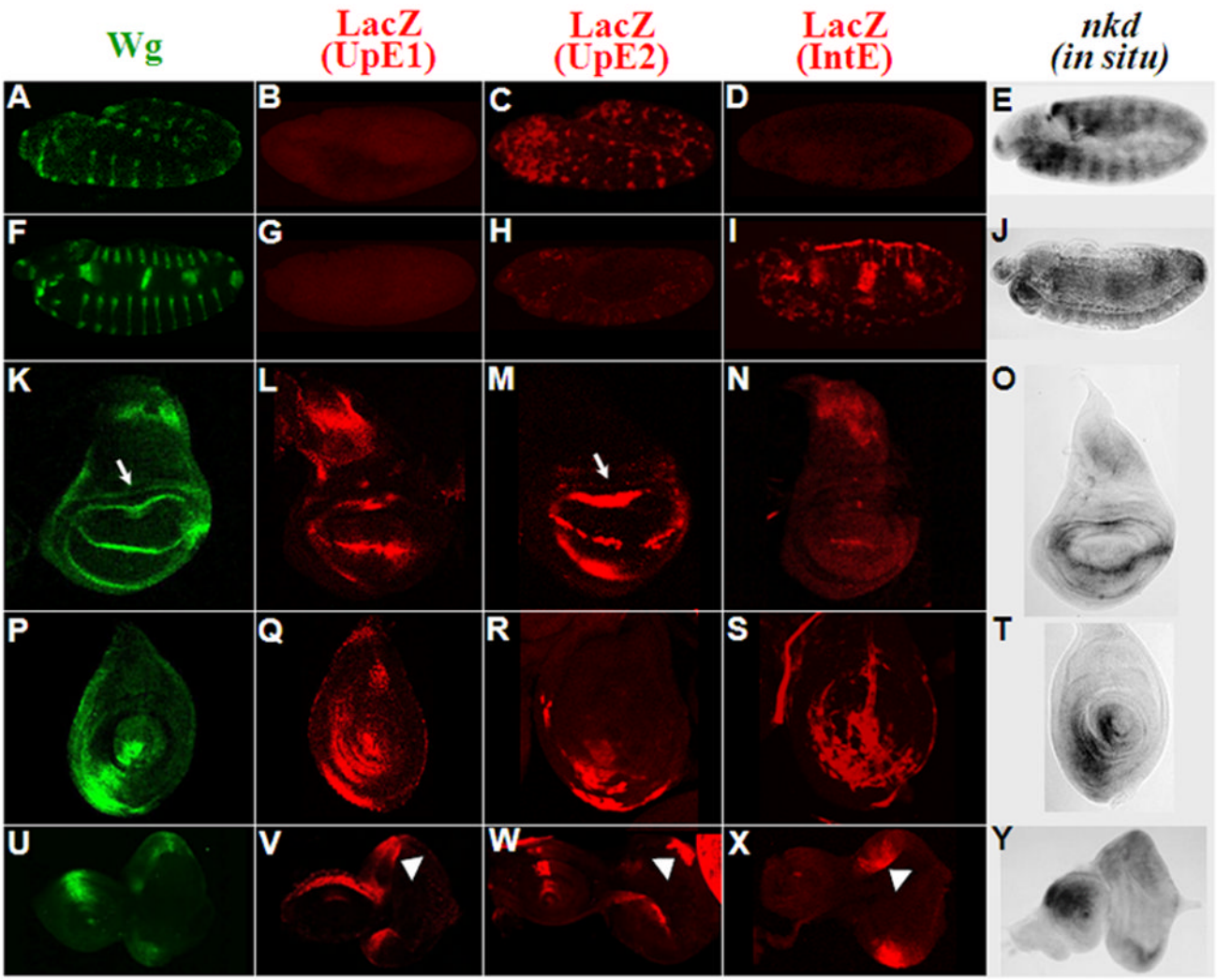

Fig. 3. *nkd*-WRE reporter transgenes are expressed in partially overlapping patterns similar to *nkd* transcript distribution

The patterns of Wg protein are shown in green, the LacZ patterns of UpE1, UpE2 and IntE reporter transgenes shown in red while *nkd* transcripts are in grey. Patterns are shown for embryos at stage 11 (*A–E*), and stage 14 (*F–J*). Late third instar wing (*K–O*), leg (*Q–S*) and eye-antennal (*U–Y*) imaginal discs are also shown. Arrows indicate the proximal ring of Wg expression (K) and faint lacZ expression in the same region of the UpE2 reporter (M). LacZ expression in eye imaginal discs is marked with arrowheads (V–X). The WRE reporters show overlapping expression domains containing a subset of the endogenous *nkd* pattern. Three independent lines of each WRE reporter showed similar results.

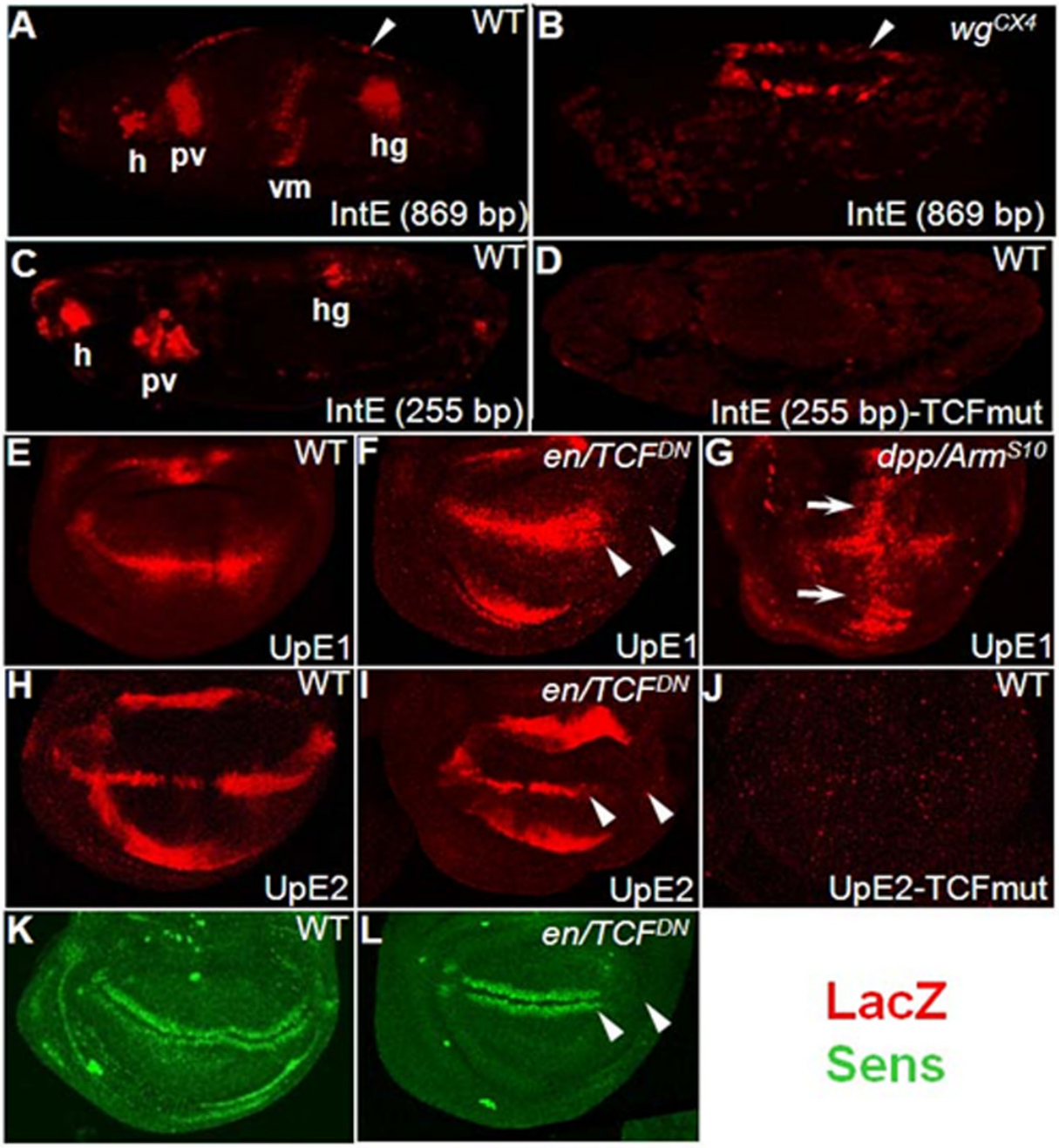

Fig. 4. The *nkd*-WRE reporters are positively regulated by Wg signaling

(*A*) Stage 14 embryo containing the *nkd*-IntE reporter stained for LacZ (red). Several expression domains consistent with positive regulation by Wg signaling are evident, including regions of the head (h), proventriculus (pv), visceral mesoderm (vm) and hindgut (hg). (*B*) IntE pattern in a *wg* mutant embryo. Most of the pattern is absent, except for the dorsal domain indicated by white arrowheads. (*C*) Stage 14 embryo with a smaller (255 bp) IntE reporter shows staining in a subset of the larger fragment. (*D*) IntE (255 bp) staining is abolished when the three TCF binding sites indicated in Fig. 2B are mutated. (E–L) The *nkd*-UpE1 and UpE2 WREs require Wg signaling in late third instar wing imaginal discs. (F, I, L) Expression of a dominant negative form of TCF (TCF^{DN}) in the posterior compartment of the wing pouch (via *En*-Gal4; marked

with arrowheads). TCF^{DN} inhibits expression of UpE1 (F), UpE2 (I) and the Wg readout Sens (L). The broader expression of lacZ in the anterior compartment of UpE1 discs (F) is likely due to distortion of disc morphology caused by TCF^{DN} expression. The slightly elevated expression of lacZ in the posterior compartment of UpE2 discs (H) is not always observed (see Fig. 3M). (G) Expression of a stable form of Arm (Arm^{S10}) along the anterior/posterior boundary of the wing pouch (via *Dpp-Gal4*; white arrows) results in marked expansion of *nkd*-UpE1 expression. The decrease in lacZ expression at the dorsal/ventral boundary is likely due to distortion of patterning in the *Dpp/*Arm^{S10} discs. (J) Mutation of the two TCF binding sites in UpE2 (the same ones indicated in Fig. 2A) abolishes reporter expression in the pouch and hinge regions of the wing imaginal discs. For the TCF mutant constructs, three independent lines were examined with identical results as those shown.

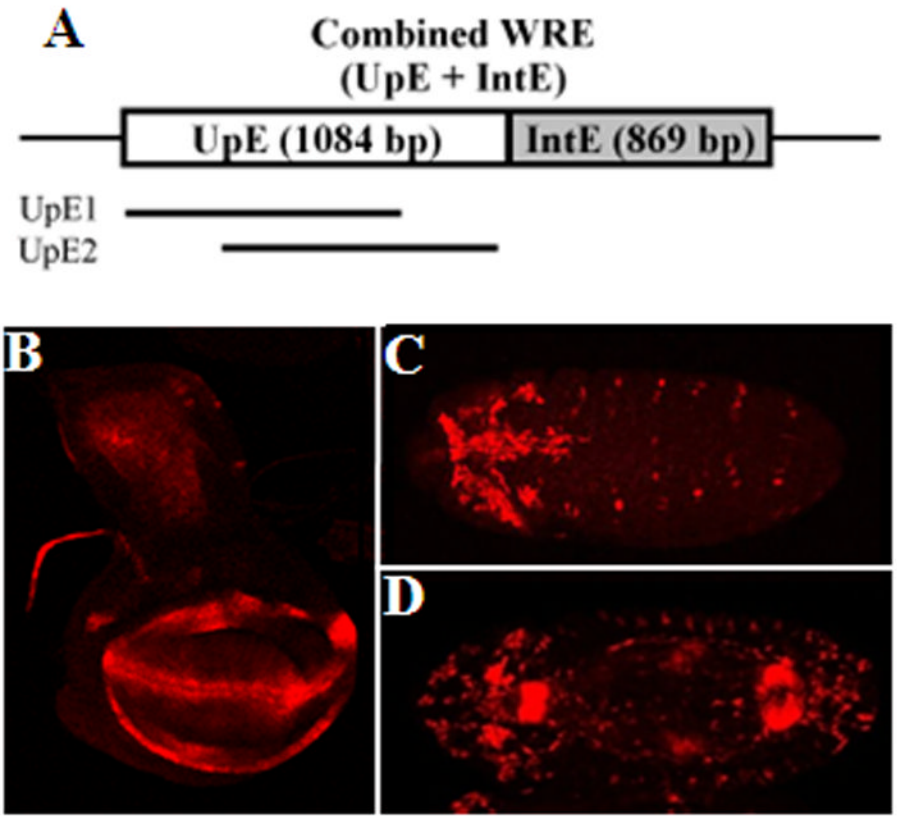

Fig. 5. The combination of UpE and IntE largely recapitulates the endogenous *nkd* pattern in late larval third instar wing imaginal discs but not in embryos

(A) The combined WRE contains the overlapping regions of UpE1 and UpE2 upstream of the 869 bp IntE in the pH-Pelican lacZ vector. (B) The expression of the combined WRE reporter in the wing disc is very similar to the endogenous *nkd* pattern (Fig. 3O) except for the proximal ring in the hinge (arrow in Fig. 6C). The combined reporter appears to be the sum of the three individual WRE reporters in regard to spatial pattern (compare with Fig. 3L –N). In regard to expression level, the combined reporter is greater in the wing hinge and pouch. The decrease gain of the confocal lasar in this image makes the notum staining less apparent (compare Fig. 5B to Fig 3L). (C, D) Ventral views of stage 11 (C) and stage 14 (D) embryos. The pattern is additive of the UpE2 and IntE WREs (Fig. 3C, I and Fig. 4A) and does not fully recapitulate the endogenous *nkd* pattern (Fig. 3E, J).

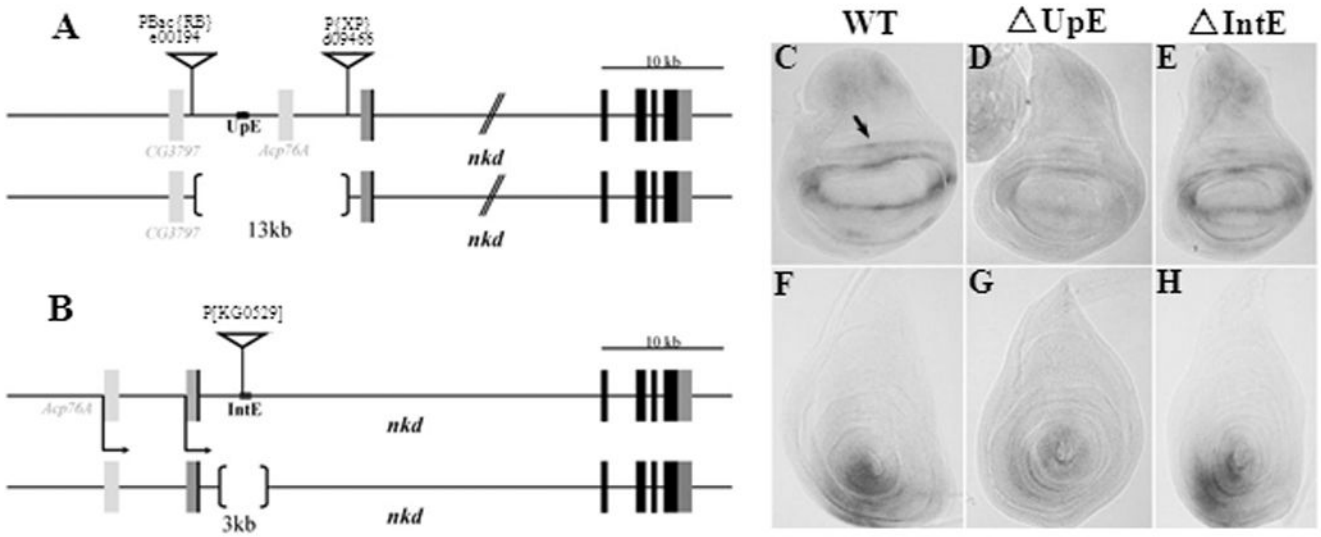

Fig. 6. Deletion of IntE does not affect *nkd* expression, but a large deletion removing UpE reduces *nkd* expression in wing and leg imaginal discs

(A, B) Cartoon of the Δ*UpE* and Δ*IntE* deletions. See Materials and Methods and Supplemental Fig. 3 for details of the deletion construction. (C–H) *nkd* transcripts in wing (C–E) and leg (F–H) imaginal discs from *+/Df(3L)ED4782* (C, F) Δ*UpE/Df(3L)ED4782* (D, G) and Δ*IntE/Df (3L)ED4782* (E, H) transheterozygotes. *Df(3L)ED4782* is a large deficiency removing the entire *nkd* locus. No noticeable decrease of *nkd* expression is detected from imaginal discs (E, H) or embryos (data not shown) when IntE is deleted. Δ*UpE/Df(3L)ED4782* transheterozygotes showed no decrease in *nkd* expression in the embryo (data not shown) but displayed a marked reduction in the wing and leg imaginal discs (D, G). This reduction was consistently observed in three independent *in situ* analyses and was also confirmed by qRT-PCR (see text).

Table 1

Summary of lacZ expression of the UpE1, UpE2 and IntE *nkd*-WRE reporters. The relative strength of expression in several tissues is indicated. All imaginal discs are from late third instar larva. See text for more details.

Tissues	*nkd*-WREs		
	UpE1	UpE2	IntE
Early embryos (stage 10–12)	−	+	−
Late embryos (stage 13–14)	−	−	+
Eye imaginal discs	+	+	+
Antennal imaginal discs	+	++	−
Leg imaginal discs (epithelia)	++	+	+/−
Leg disc (peripodal membrane)	+/−	+	++
Wing disc (notum)	+	−	+
Wing disc (D/V boundary)	++	++	+
Wing disc (hinge-distal ring)	+	++	−